Physical Aging of Polycarbonate: Enthalpy Relaxation, Creep Response, and Yielding Behavior

J. M. Hutchinson,* S. Smith, B. Horne, and G. M. Gourlay

Department of Engineering, King's College, University of Aberdeen, Aberdeen AB24 3UE, U.K.

Received September 2, 1998; Revised Manuscript Received March 30, 1999

ABSTRACT: The effect of annealing polycarbonate at 125 °C ($\approx T_g - 20$ K) for aging times up to almost 2000 h has been investigated by differential scanning calorimetry, and the kinetics of the enthalpy relaxation process are compared with the effects of aging at the same temperature on the creep response and on the yield behavior. The enthalpy relaxation is analyzed by the peak shift method, and the following kinetic parameters are obtained: nonlinearity parameter $x = 0.46 \pm 0.02$; apparent activation energy $\Delta h^* = 1160$ kJ mol^{-1}; nonexponentiality parameter β is in the range $0.456 < \beta < 0.6$. The similarities and/or differences between these results and others quoted in the literature are discussed. The creep response is analyzed by the commonly accepted procedure of horizontal and vertical shifting of deflection vs log(creep time) curves, and a shift rate of $\mu = 0.87$ is obtained, with an excellent master curve. It is shown that a similar shift rate for enthalpy relaxation can be defined, and a value of $\mu_H = 0.49$ is found. The difference between these two shift rates suggests that the time scales for the aging process are different when probed by the two techniques of creep and enthalpy relaxation. Similarly, it is found that the yield stress of annealed samples depends on log(aging time) in quite a different way from its dependence on log(strain rate), and it is argued that this provides further support for the contention that the time scales and rates of physical aging will be different when probed by different techniques.

1. Introduction

The process of annealing amorphous materials, including polymers, in a temperature range below their glass transition temperature (T_g) is well-known to result in changes in their structure and properties. This phenomenon, often referred to as physical aging,[1−4] occurs because an amorphous material at a temperature below T_g is in a glassy, nonequilibrium state which, on annealing at constant temperature, will approach with time an equilibrium state at that temperature. This equilibrium state will be defined by invariant values of quantities characterizing the structure and properties of the material, and the physical aging behavior can be followed by the changes in these quantities as they approach their limiting equilibrium values.

It is widely held that the changes in properties, and in particular in the present context in the mechanical properties, of materials during physical aging are related to the structural changes taking place. The details of this relationship between structure and properties during physical aging remains somewhat unclear, though. Indeed, so also does the relationship between different quantities used to measure the structural changes. For example, the question of whether enthalpy and specific volume age at the same rate, or of which, if either, correlates directly with the aging of creep or stress−relaxation behavior, is very much open to debate (see, for example, the discussion of this in ref 5).

In a recent study of physical aging in poly(vinyl acetate) by dynamic mechanical, enthalpic and dilatometric experiments,[5] it was concluded that there are in general different time scales for aging as monitored by each of these three techniques. In the present work, we further examine this suggestion by monitoring the physical aging of polycarbonate by enthalpy relaxation and by the low strain torsional creep response. In addition to a detailed examination of each of these relaxation processes, we have studied the effect of aging on the yield behavior of polycarbonate for specimens tested in uniaxial tension at constant extension rate. The rates of physical aging as measured by enthalpy, creep, and yield will be compared and discussed in the context of the relationship between structure and properties during physical aging.

* To whom correspondence should be addressed: Telephone: +44 1224 272791. Fax: +44 1224 272497. E-mail: j.m.hutchinson@eng.abdn.ac.uk.

2. Experimental Section

2.1. Materials and Specimens. The polycarbonate of bisphenol A used in this work was obtained as a commercial material from two sources, both based upon the same resin. One was in the form of extruded rod, 40 mm diameter, from which specimens for differential scanning calorimetry (DSC) and for creep experiments were machined. The rod was extruded using extrusion grade Lexan (GE Plastics) polycarbonate by Ensinger Ltd, the extruded product having the tradename Tecanat. The other was extruded sheet (Lexan 9030, GE Plastics), nominally 5 mm thick, from which the specimens for tensile testing were machined. Lexan 9030 is a standard extrusion grade with no UV stabilization and without any surface treatment and has a manufacturer's quoted molecular weight of $\bar{M}_w = 31\,000$.

The extrusion of the solid rod (40 mm diameter) is a much slower process than the extrusion of sheet, and hence the material remains at the extrusion temperature for longer periods of time in the former case. This can have an effect on the detailed structure of the material. However, DSC scans on samples of each of the two materials showed very similar glass transitions, both having a breadth of transition (endset-onset) of 11 ± 1 K and a specific heat capacity increment (ΔC_p) of 0.26 ± 0.01 J g^{-1} K^{-1}, and with a difference of only about 3 K in the glass transition temperature measured at the midpoint of ΔC_p, on heating at 10 K min^{-1} immediately following cooling at 20 K min^{-1}. These observations imply that the various results from the polycarbonates obtained from the two sources can be compared.

10.1021/ma981391t CCC: $18.00
Published on Web 07/13/1999

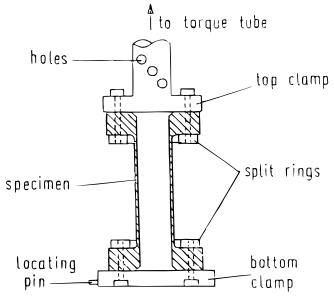

Figure 1. Schematic (not to scale) illustration of the torsional creep specimen.

For the DSC experiments (enthalpy relaxation), the extruded rod was cut axially into four equal segments, and a 5 mm diameter rod was turned from the central region of each of these segments. These 5 mm diameter rods were then parted on a lathe, using a sharp parting tool, to give disks of approximately 0.5 mm thickness. The choice of 5 mm diameter was to provide a neat fit inside standard aluminum pans used in the Perkin-Elmer DSC-4, while the choice of 0.5 mm thickness gave DSC samples of approximately 12 mg mass.

For the torsional creep experiments (see below), thin-walled cylindrical specimens with integral flanges at each end were machined from the extruded rod (refer to Figure 1). The flanges were 35.0 mm diameter and 6.0 mm thick, each with four drilled holes of 3.5 mm diameter on a 20.0 mm pitch circle diameter for clamping to the creep apparatus. A 10 mm diameter central hole was drilled the full length (52.0 mm) of the specimen, a mating mandrel was inserted, and then the specimen supported on the mandrel was turned on a lathe to give a wall thickness of 0.2 mm along the "working length" (40.0 mm) of the specimen. This thin-walled cylindrical geometry ensures a uniform shear stress in the sample when subjected to a torque, with the ratio of maximum to minimum shear stress differing by less than 5% from unity. The nominal machining tolerance was 0.01 mm, which would imply a possible inaccuracy of 5% in the wall thickness, with a corresponding error in the compliance. However, since absolute values of compliance were not required in this work investigating isothermal changes on aging, this thin-walled geometry was adopted both for the uniformity of stress and also for the rapidity with which the specimen could adapt to temperature changes, while minimizing thermally induced stresses, when the aging process was initiated.

The tensile test specimens were machined directly from the extruded sheet in the form of dumbbells, with their shape prescribed by the relevant British Standard,[6] using a CNC mill and high-speed router−cutter. The specimen axis was always in the same direction relative to the extrusion direction for the sheet, and the gauge portion had a length of 60.0 ± 0.5 mm, a width of 10.0 ± 0.1 mm, and a thickness of the extruded sheet of 4.82 ± 0.04 mm.

2.2. Enthalpy Relaxation Experiments. The measurements of enthalpy relaxation were made using a Perkin-Elmer differential scanning calorimeter, model DSC-4, with a thermal analysis data station and a liquid nitrogen controlled cooling accessory with the block set at −30 °C. The baseline was checked daily, and temperature scale calibration was made at regular intervals using the melting transition of pure indium. The purge gas was dry nitrogen at a controlled flow rate.

The polycarbonate samples, prepared as described above, weighed on a microbalance, and sealed in standard aluminum pans, were subjected to the following thermal treatment. Initially, all samples were heated in the DSC (at 20 K min^{-1}) to a temperature of 160 °C, just above the glass transition temperature of polycarbonate ($T_g \approx 145$ °C), to eliminate their previous thermal history. They were then cooled at 10 K min^{-1} to the annealing temperature T_a, which was selected as 125 °C, i.e., 20 °C below the nominal T_g.

Samples which were to be annealed for times longer than 4 h were transferred, immediately after this controlled cooling, into an electrically heated oven controlled at the annealing temperature, 125.0 ± 0.2 °C. To further ensure temperature stability, and to allow easy identification of any sample, they were placed inside the oven onto a square aluminum block, approximately 200 mm square and 8 mm thick, which had been drilled with a 7 × 7 square array of shallow holes of a suitable diameter for accepting the aluminum pans. The identity of each sample was recorded with its location in this array, together with its time and date of entry into the oven. By using multiple samples (about 15 in total), a wide range of annealing times, up to almost 2000 h, could easily be achieved. The temperature of the aluminum block was continuously monitored with a copper−constantan thermocouple.

For annealing times of 4 h and less, the samples were annealed directly in the DSC. It is impractical to use the DSC as an oven for longer annealing times; furthermore, it would then not be possible to make the regular baseline checks and temperature calibrations. No discontinuity was observed between results obtained for less than and greater than 4 h, indicating that the two annealing procedures (in the oven and in the DSC) are equivalent.

Following the annealing treatment, for the length of time selected for a given sample such that the required range of annealing times (t_a) was covered at approximately equal intervals of log t_a, the sample was returned to the DSC (except for those with $t_a \leq 4$ h, which remained in the DSC) set at 125 °C, cooled at 10 K min^{-1} to 60 °C, and then immediately reheated at 10 K min^{-1} to 160 °C to obtain the first (annealed) scan. The same sample was then cooled at 10 K min^{-1} to 60 °C and again reheated at 10 K min^{-1} to 160 °C to obtain the second (unannealed, or reference) scan. After these two scans, the sample could be used again for further annealing times. The excellent superposition of the aged and reference scans and of scans corresponding both to a variety of aging times and also to multiple use of samples indicates that the sample attains a reproducible state each time it is heated above T_g, to 160 °C.

A further set of experiments was required in order to determine the apparent activation energy for enthalpy relaxation. This can be found (see theoretical section 3.1 below) from the dependence of the glass transition temperature (or fictive temperature) on the cooling rate. Accordingly, the following procedure was used for these experiments, the so-called constant cooling rate experiments.

A single sample was used throughout. The sample was initially heated in the DSC at 10 K min^{-1} to 160 °C in order to erase its thermal history. It was then cooled at 80 K min^{-1} to 60 °C and immediately reheated at 10 K min^{-1} to 160 °C, the heating scan being recorded. This procedure was repeated using cooling rates of 40, 20, 10, 5, 2.5, 1.2, 0.5, and 0.1 K min^{-1}, each time reheating from 60 to 160 °C at 10 K min^{-1} immediately after the cooling stage. The heating scans obtained after the various cooling rates permit both the determination of T_g as a function of cooling rate and also an estimation of the distribution of relaxation times (see theoretical section 3.1 below). The use of just a single sample for these experiments is important in reducing experimental error because the changes that are being measured, for example in T_g, are rather small.

2.3. Creep Experiments. The creep specimen, in the form of a thin-walled tube with a flange at each end as described above, was clamped in the torsional creep apparatus which has been described in some detail elsewhere.[7] This apparatus, shown schematically in Figure 2, consists essentially of a coil suspended between the poles of a permanent magnet and fixed rigidly to a torque tube, the other end of which is clamped to the flange of the specimen. The other flange of the specimen is clamped rigidly to the frame of the apparatus, and the coil and torque tube are counterbalanced using a sliding weight on a freely pivoting lever. A constant current from a Farnell stabilized power supply is passed through the coil in order to provide a constant torque on the specimen for the creep experiment. The angle of twist of the specimen which results is measured by reflecting a light beam off the concave mirror fixed rigidly to the torque tube, the focused image being

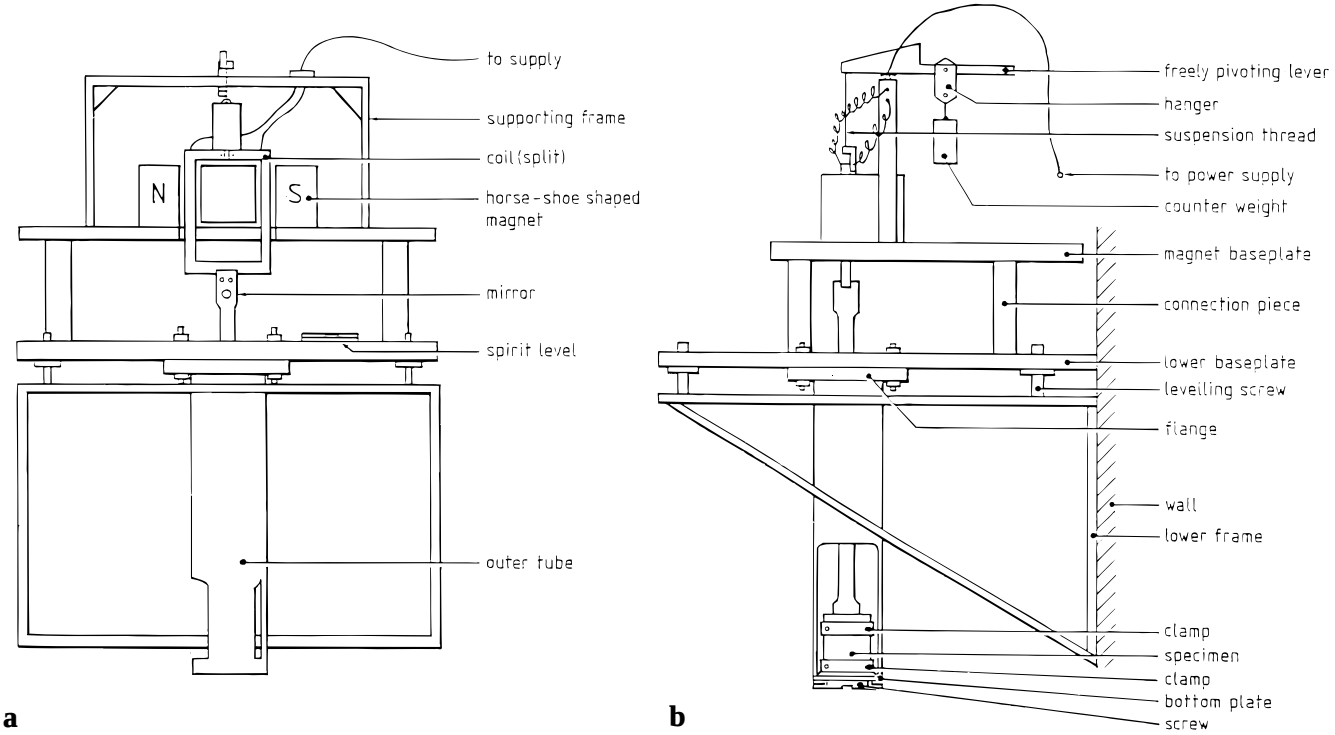

Figure 2. Front elevation (a) and side elevation (b) of torsional creep apparatus.

followed continuously by the photocell of a Graphispot chart recorder at several meters distance from the mirror.

The torsional creep apparatus is designed such that the specimen can be immersed in a temperature controlled bath so that the creep response can be followed over a range of temperatures. The procedure adopted for the purposes of monitoring the physical aging at 125 °C was as follows. Before each aging experiment, the specimen was immersed in a bath of silicone oil at 160 °C for about 15 min in order to erase its previous thermal history (a process of rejuvenation). The sample response was monitored during this stabilization period at 160 °C and was observed to settle within less than 5 min to oscillations, caused by the circulation of the silicone oil around the specimen in the thermostated bath, around a constant mean position. Since the specimen has a very low modulus at this temperature (in the rubbery region, hence the oscillations mentioned above), we take this to imply that the internal stresses have relaxed to an insignificant level compared with the stress to be applied at a lower temperature sufficient to cause measurable creep to occur. To initiate the aging process, the bath at 160 °C was removed and rapidly replaced with another temperature controlled bath (Techne, TE−160) set at 125.0 ± 0.2 °C. The moment of immersion of the specimen into the bath at 125 °C was taken as the initial time for aging.

The thin-walled geometry of the specimen ensured that thermal stresses induced by the quench were minimized and that the aging temperature was established rapidly. A dummy sample immersed in the silicone oil for long periods of time exhibited no significant interaction between the silicone oil and the polycarbonate sample. Indeed, the inertness of silicone oil to another glassy polymer, polystyrene, was previously utilized to construct a density gradient column from silicone oils of different densities for the "in situ" monitoring of density changes of polystyrene during physical aging.[8]

Creep experiments at low strain (<0.25%) were performed at approximately equal logarithmic aging time intervals according to the protocol of Struik.[1] This limits the creep time to one-tenth of the aging time, such that the specimen can be considered to be in a quasi-isostructural state throughout any creep test, and the creep test is followed by a recovery period of approximately 10 times the creep duration, thus allowing sufficient recovery to occur such that it has no significant influence on the subsequent creep curves.

The creep behavior is recorded as the displacement of the photocell of the chart recorder on a chart set to run at constant linear speed. Data are then taken from the chart and transposed onto the more useful plot of deflection as a function of logarithmic creep time.

2.4. Tensile Testing. The samples machined to the required dimensions as described above were first all placed in an air-circulating oven and heated to 160 °C, at which temperature they were held for a period of 1 h to ensure uniformity of temperature and erasure of their previous thermal history. To ensure that the specimens did not deform during this heat treatment, they were placed flat on a smooth aluminum plate inside the oven. The original extruded sheet will certainly contain both elastic stresses and frozen-in strains, or orientation. The elastic stresses generally relax rather rapidly, and would be negligible after 1 h at 160 °C. The frozen-in strains, or orientation, on the other hand, may persist for long annealing times, but would be significantly reduced after a period of 1 h at 160 °C, although no direct birefringence measurements were made.

To initiate the aging process, the specimens were removed from the oven at 160 °C and placed on a flat aluminum plate in a temperature controlled oven at 125.0 ± 0.2 °C (the same oven that was used for the DSC specimens in the enthalpy relaxation experiments). It is known that this process of cooling through the glass transition will introduce some thermal stresses, as also will the subsequent cooling from the annealing temperature to the ambient test temperature. The former will relax relatively rapidly, and in a 5 mm sheet may be anticipated to be on the order of 5 MPa maximum. The latter involves a much slower cooling rate, as the specimens are cooling by convection in essentially still air, and hence the thermal stress level will be correspondingly small. In comparison with the stress levels on the order of 65 and 50 MPa in the yield and drawing processes, respectively, for polycarbonate, these internal stresses, which will contribute in essentially the same way for all the annealed specimens tested, may be considered as not having a significant influence on our interpretation of the results.

At the required aging time, selected at approximately equal logarithmic intervals up to more than 2000 h, samples were removed from the oven and allowed to cool in air to ambient temperature (≈23 °C). They were then mounted between the wedge grips of a universal testing machine (Instron 1185) set

with a constant cross-head speed of 2 mm min^{-1}, a full scale load of 5 kN, and a proportional chart drive set at 25:1. Each tensile test was continued beyond the point at which shear yielding occurred, until a neck had clearly formed (unless fracture intervened) and the load had become almost constant.

A further set of experiments was conducted on "as received" samples, i.e., with the thermal history of the extruded sheet (probably a year or more at room temperature) and without any rejuvenation, to examine the strain rate dependence of the yielding of polycarbonate. For these experiments, cross head speeds of 0.02, 0.2, 2, 20, and 200 mm min^{-1} were used, reducing the proportional chart drive to 5:1 for the highest strain rate.

3. Theory and Data Analysis

3.1. Enthalpy Relaxation. The procedure adopted here for the analysis of the DSC data follows a well-recognized approach. It is assumed, as is common practice, that the relaxation time(s) for enthalpy relaxation depends on both the temperature (T) and the structure of the glass, identified by its fictive temperature (T_f), according to the so-called Tool–Narayanaswamy–Moynihan[2,9–11] or TNM equation

$$\tau = \tau_o \exp\left[\frac{x\Delta h^*}{RT} + \frac{(1-x)\Delta h^*}{RT_f}\right] \qquad (1)$$

where τ_o is the value of τ in equilibrium at infinitely high temperature, Δh^* is the apparent activation energy for enthalpy relaxation, and x ($0 \le x \le 1$) is the nonlinearity parameter[12,13] identifying the relative contributions of temperature and structure to the relaxation time(s).

It should be pointed out here that the TNM equation is not without its detractors, nor is it the only formalism that could be adopted. The reader is referred to ref 2 for an excellent overview of the various approaches, including in particular the analysis originally developed for equilibrium conditions by Adam and Gibbs[14] and subsequently extended by other workers[2,15] to include nonequilibrium, and hence nonlinear, effects. We choose here the TNM model for our data analysis because this is the formalism adopted in earlier work (e.g. refs 12 and 13) and incorporating the parameters x and Δh^*, the values of which may usefully be compared for different glass-forming systems in an attempt to rationalize relaxation processes at the glass transition. A discussion of the implications of this choice and of the relative merits of TNM or Adam–Gibbs is deferred to section 5.3.

Equation 1 is written for a single relaxation time; it is well-known, though, that an indispensable feature of the kinetics of enthalpy relaxation is the inclusion of a distribution of relaxation times.[16] This could be included in the analysis by subscripting τ_i and τ_{oi} to represent the ith element of a discrete distribution as in the KAHR model[12] or by the use of a stretched exponential response function

$$\phi(t) = \exp[-(t/\tau)^\beta] \qquad (2)$$

to simulate a continuous spectrum, in which τ is given by (1) and β ($0 \le \beta \le 1$) is a parameter inversely related to the width of the spectrum.

For the three-step thermal cycles used here, involving (i) cooling at constant rate q_1 until the annealing (or aging) temperature T_a is reached, (ii) annealing at T_a for time t_a such that the enthalpy decreases by an amount $\bar{\delta}_H$, and then (iii) reheating at constant rate q_2 until equilibrium is again established at high temperature, a peak is observed in the DSC scan on reheating. The temperature T_p at which this endothermic peak appears is a function of the three experimental variables (q_1, $\bar{\delta}_H$ and q_2), and the dependence of T_p on any one of these individually, while the others are held constant, is the basis of the so-called peak shift method that is used here.[17,18] For experimental reasons, it is most convenient to determine the dependence of T_p on $\bar{\delta}_H$ for constant values of q_1, T_a and q_2, from which one can define a normalized (dimensionless) shift $\hat{s}(\bar{D})$ given by

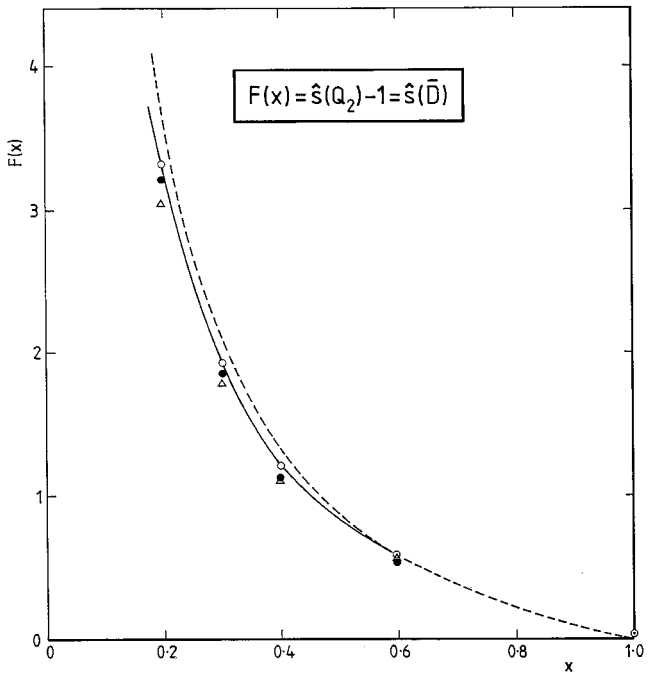

Figure 3. Theoretical dependence of $\hat{s}(\bar{D})$ on the nonlinearity parameter x for different distributions: dashed line, single relaxation time; open circles, single-box discrete distribution 2 decades wide; filled circles, double-box discrete distribution 4 decades wide; triangles, stretched exponential response function with $\beta = 0.456$.[17,18]

$$\hat{s}(\bar{D}) = \Delta C_p \left(\frac{\partial T_p}{\partial \bar{\delta}_H}\right)_{q_1,T_a,q_2} \qquad (3)$$

where $\Delta C_p = C_{pl} - C_{pg}$ is the difference between the specific heat capacities of the equilibrium liquid and of the glass. This normalized shift is therefore determined from a set of experiments involving samples aged for different times t_a such that a range of $\bar{\delta}_H$ values is covered. The enthalpy loss on aging, $\bar{\delta}_H$, is found simply from the area difference under the DSC curves for the aged and for the reference scans.

The advantage of the peak shift method[17,18] lies in the observation that the shift $\hat{s}(\bar{D})$ defined by (3) is a strong function of the nonlinearity parameter x but is almost independent of the distribution of relaxation times. The dependence of $\hat{s}(\bar{D})$ on x has been determined theoretically[17] for a wide range of distributions and is shown in Figure 3. The experimental procedure is thus to determine $\hat{s}(\bar{D})$ according to eq 3 and then from Figure 3 (the master curve) to find x, which is rather precisely determined, perhaps ± 0.02, independent of the distribution.

The evaluation of the apparent activation energy Δh^*, introduced in (1) above, requires the set of experiments in which the sample is cooled at different constant rates

before immediately scanning in the DSC. The dependence of the glass transition temperature T_g or of the fictive temperature T_f (these are the same if the sample is unannealed, i.e., reheated immediately after cooling, as is the case here) on the cooling rate q_1 may be written[11,12]

$$\frac{d(\ln[|q_1|])}{d[1/T_f]} = -\frac{\Delta h^*}{R} \tag{4}$$

The fictive temperature for a given cooling rate is found by the "equal area" method or its algebraical equivalent,[11,19] and the apparent activation energy is then evaluated from the slope of a plot of $\ln[|q_1|]$ vs $[1/T_f]$.

The same set of cooling rate experiments may be used to estimate the nonexponentiality parameter β, introduced in (2). For each cooling rate, the heating scan made immediately afterward in the DSC displays a small endothermic peak, a so-called upper peak.[20] The normalized upper peak height, defined as

$$C_{p,u}{}^N = \frac{C_{p,u}}{\Delta C_p} \tag{5}$$

where $C_{p,u}$ is the magnitude of C_p at the upper peak, depends on the ratio of cooling rate q_1 to heating rate q_2, on the parameter β, and, to a lesser extent, on the nonlinearity parameter x. The theoretical dependence of $C_{p,u}{}^N$ on $\log [|q_1|/q_2]$ for various combinations of values of β and x has been determined previously,[20] and a comparison with experimental data, for which x has previously been determined independently of β by the peak shift method, allows an estimate of β to be made.

The peak shift method, the cooling rate experiments, and the normalized upper peak height thus allow the determination of each of the three parameters which characterize the kinetics of enthalpy relaxation, namely the nonlinearity parameter x, the apparent activation energy Δh^*, and the nonexponentiality parameter β, respectively.

3.2. Creep Behavior. The shear strain in the thin-walled cylindrical sample is given by

$$\gamma(t) = \frac{r}{2Ll}\delta(t) \tag{6}$$

where r is the radius (5.0 mm) and l is the working length (40.0 mm) of the sample, L is the optical lever (distance from mirror on torque tube to photocell of chart recorder, 8.16 m), and $\delta(t)$ is the deflection measured on the chart recorder at creep time t. Thus, for the experimental arrangement used here, $\gamma(t) = 7.66 \times 10^{-6} \times \delta(t)$, when $\delta(t)$ is measured in units of millimeters. Since the maximum deflection in these creep experiments was 250 mm, the maximum strain in the specimen was therefore on the order of 0.2%, well within the linear viscoelastic regime. Furthermore, since δ could be measured to approximately 0.1 mm, the precision of these creep data may be estimated to be on the order of one microstrain.

The applied shear stress is constant, and may be calculated from the measured current applied to the coil, the specimen dimensions, and the coil constant, previously determined by calibration with a metallic sample of known modulus.[7] The creep compliance $J(t)$ is therefore directly proportional to the deflection $\delta(t)$, and it suffices to represent the creep behavior in terms of the time dependence of the deflection δ.

The creep compliance may be written as

$$J(t) = J_U + \Sigma\Delta J_i[1 - \exp\{-t/\tau_{ci}\}]; \quad \Delta J = \Sigma\Delta J_i \tag{7}$$

for a discrete distribution of creep relaxation times τ_{ci}, each with a weighting factor ΔJ_i, or as

$$J(t) = J_U + \Delta J[1 - \exp\{-(t/\tau_c)^\beta\}] \tag{8}$$

for a continuous spectrum approximated by a stretched exponential function with exponent β and characteristic creep relaxation time τ_c. The exponent β may or may not be the same as that characterizing the spectrum of enthalpy relaxation times [refer to (2)]; this is an open question. In (7) and (8), J_U is the unrelaxed compliance and ΔJ is the relaxation strength, equal to the difference between the relaxed (J_R) and unrelaxed compliances, $\Delta J = J_R - J_U$.

The effect of physical aging on the creep compliance may be manifest in a number of ways, through its influence on any or all of the following: the unrelaxed compliance, the relaxation strength, and the spectrum of relaxation times. A systematic approach to this problem was provided by Chai and McCrum,[21] whose analysis may be summarized as follows.

(a) If the unrelaxed compliance and relaxation strength are both unaffected by aging, the only effect being on the distribution of relaxation times, then during aging the creep curves will be shifted horizontally along the logarithmic creep time scale, and will superpose to form a master curve if the system is thermorheologically simple (i.e. if all the τ_{ci} in (7) depend in the same way on the aging time or if β in (8) remains constant on aging). The horizontal shift $\log a$ of this time−aging time superposition gives a shift factor a which depends on the aging time in a way analogous to the temperature dependence of the shift factor a_T in time−temperature superposition.[22]

(b) If, in addition to its effect on the time scale as in (a) above, aging causes a change (usually a reduction) in the limiting compliances J_U and J_R, but the relaxation strength ΔJ remains invariant on aging, then time−aging time superposition can be achieved by means of a combination of horizontal shifting (giving a shift factor a) and vertical shifting (giving a shift factor c as the ratio of the aged and unaged, or reference, values of either J_U or J_R).

(c) As was pointed out by Chai and McCrum,[21] the assumption in points a and b above that the relaxation strength ΔJ remains invariant may be rather sweeping, and they proposed an alternative procedure which eliminates the effect of the shift factor c. If the creep rate dJ/dt is plotted on a logarithmic scale as a function of log creep time, then these differentiated creep curves should superpose, for a thermorheologically simple system, by means of a horizontal shift of $\log a$ and a vertical shift of $(\log a - \log b)$, where the shift factor b defines the change in relaxation strength ΔJ on aging.

The creep curves presented here will be examined to see to what extent a good master curve may be obtained by superposition following the shifting procedures described in each of parts a−c above.

3.3. Tensile Tests. The data analysis for the tensile tests is best illustrated by reference to typical curves such as those shown in Figure 4. The nominal stress is calculated from the force divided by the original cross-

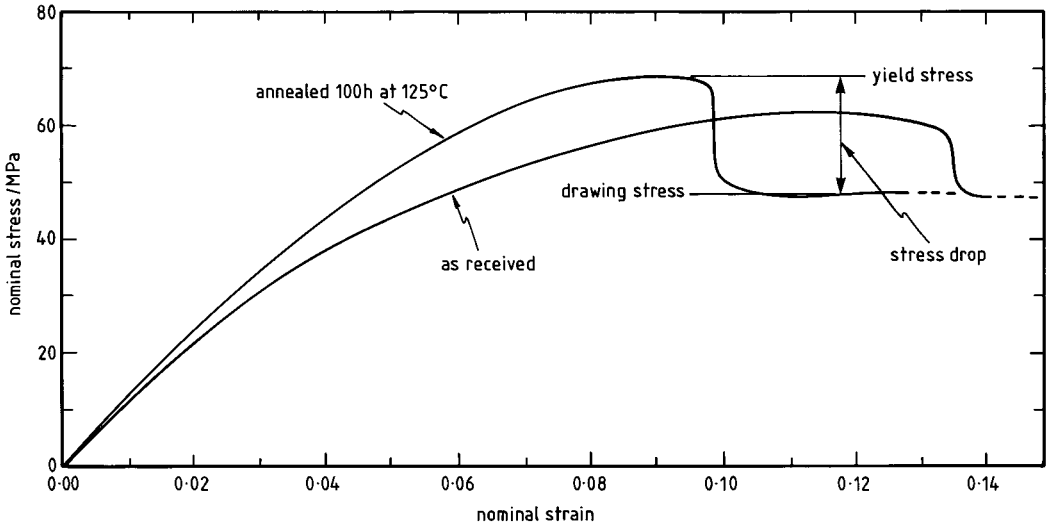

Figure 4. Typical tensile test data for polycarbonate at cross-head speed of 2 mm min^{-1} tested at room temperature.

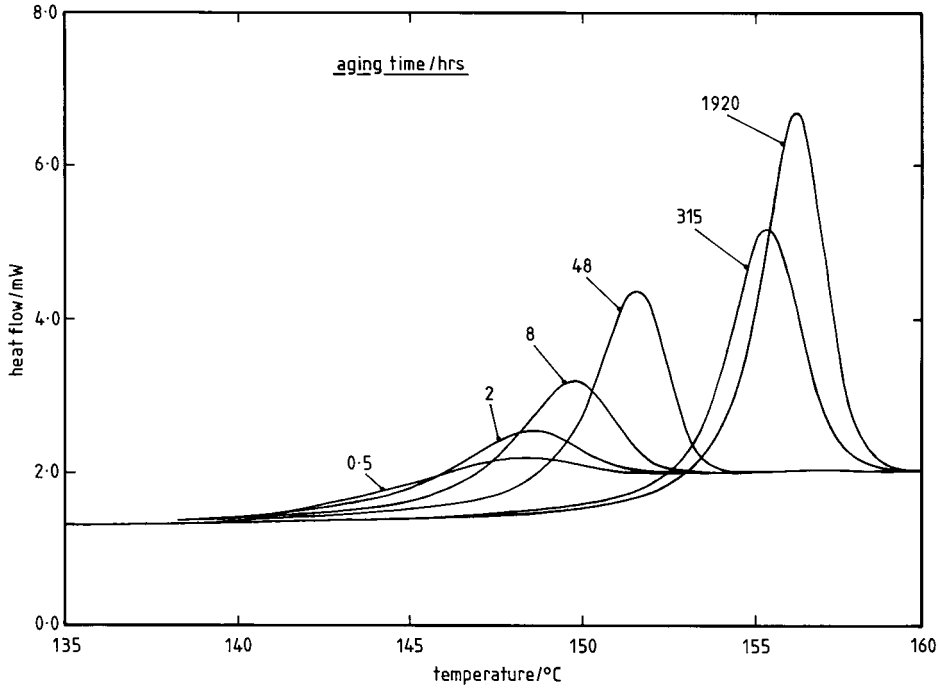

Figure 5. DSC heating scans at 10 K min^{-1} for polycarbonate samples annealed at 125 °C ($\approx T_g - 20$ °C) for the times (in hours) indicated against each curve. Note that only a part of the heating scan is shown here; the whole scan was from 60 to 160 °C.

sectional area (≈48 mm^2), and the nominal strain is calculated from the extension, measured simply as cross-head displacement, divided by the original gauge length (60 mm). The yield stress is defined as the maximum nominal stress, and the drawing stress is the approximately constant value of the nominal stress which occurs when the initial yield process is complete and corresponds to the drawing of undeformed material from the gauge length of the specimen into the neck region of approximately uniform and constant dimensions.

4. Results

4.1. Enthalpy Relaxation. A typical set of DSC traces for samples of polycarbonate annealed at 125 °C for the times indicated is shown in Figure 5. Only a part of the complete scan (from 60 to 160 °C) is shown here in order to separate the curves more clearly. From these curves, the peak endotherm temperature T_p and the enthalpy loss on aging $\bar{\delta}_H$ are obtained as a function of aging time. The latter is found from the area difference between the annealed curve and the reference unannealed curve (not shown in Figure 5), scaled appropriately for the heating rate and sample mass. The dependences of the peak temperature and of the enthalpy loss on the logarithm of the aging time are shown in Figures 6 and 7, respectively.

The usual behavior of glassy polymers can be seen here, with both T_p and $\bar{\delta}_H$ increasing linearly with log (aging time). The only deviation from this behavior is for short aging times, less than 2 h, for which the peak temperature appears to remain rather constant (as indicated in Figure 6 by the dashed line). In fact, this behavior is anticipated for sufficiently short aging times;[18,20] under these circumstances, the poorly annealed glass displays what is called an upper peak during the heating scan, which can be shown theoretically to remain invariant on annealing.[17,23] On the other

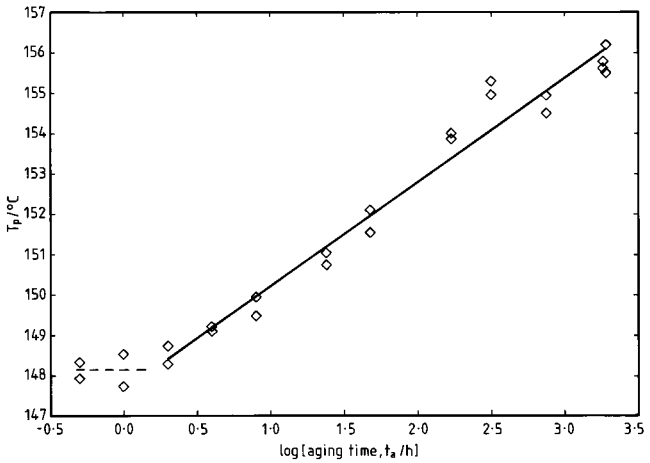

Figure 6. Dependence of the peak endotherm temperature on log [aging time] for polycarbonate samples annealed at 125 °C ($\approx T_g - 20$ °C). The full line represents a least-squares fit to the data for aging times greater than or equal to 2 h. The dashed line indicates an approximately constant peak temperature for $t_a < 2$ h.

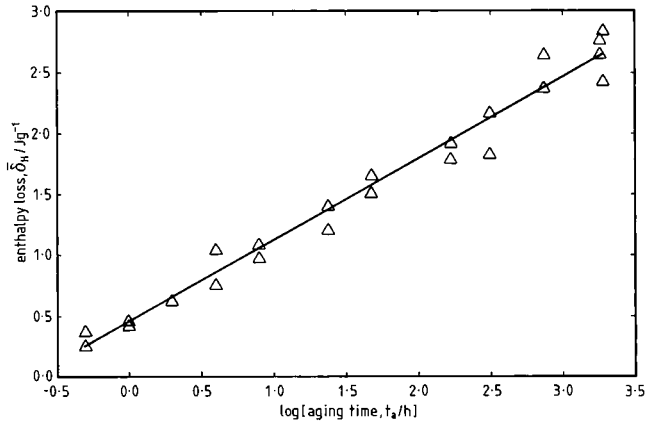

Figure 7. Dependence of the enthalpy loss during aging of polycarbonate at 125 °C ($\approx T_g - 20$ °C) as a function of log (aging time). The full line represents a least-squares fit to the data.

hand, the plot of $\bar{\delta}_H$ as a function of log(t_a) does not show this discontinuous behavior because enthalpy is being continuously lost on aging, even for rather short annealing times; it is only as a result of the kinetics of the relaxation processes during the heating scan that the invariant upper peaks appear.

The slopes of the best fit straight lines in Figures 6 and 7 give the following values for the dependences of T_p and $\bar{\delta}_H$ on log(aging time): $(\partial T_p/\partial(\log[t_a]))_{q_1,T_a,q_2} = 2.58$ K per decade and $(\partial\bar{\delta}_H/\partial(\log[t_a])_{q_1,T_a,q_2} = 0.67$ J g^{-1} per decade, with correlation coefficients of 0.969 and 0.975, respectively. This latter value is close to those obtained by others[24,25] at $T_g - 15$ K, and summarized in Table 2 of ref 3. Combining the values for these two slopes, one obtains $(\partial T_p/\partial\bar{\delta}_H)_{q_1,T_a,q_2} = 3.85$ g K J^{-1}.

Since C_{p1} and C_{pg} are both to a certain extent temperature dependent, the evaluation of ΔC_p needs to be made at a specified temperature. Here, ΔC_p was found at the fictive temperature of unannealed samples cooled at 10 K min^{-1}, and the average value from nine separate measurements was 0.258 ± 0.006 J g^{-1} K^{-1}. This can be compared, for example, with $\Delta C_p = 0.234$ Jg^{-1} K^{-1} quoted in ref 24.

The evaluation of the nonlinearity parameter x can now be made by determining the shift $\hat{s}(\bar{D})$, defined by

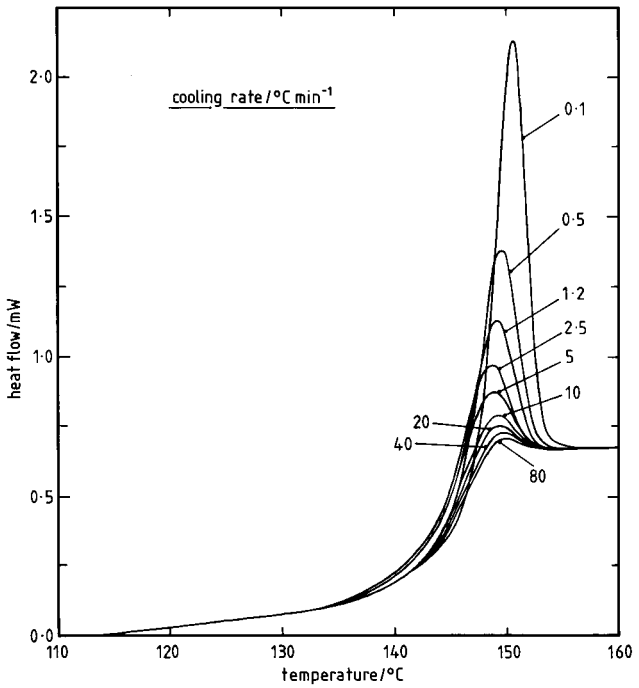

Figure 8. Heating scans at 10 K min^{-1} for polycarbonate samples cooled at the rates indicated against each curve and then immediately reheated in the DSC. Note that only a part of the complete scan from 60 to 160 °C is shown here for clarity.

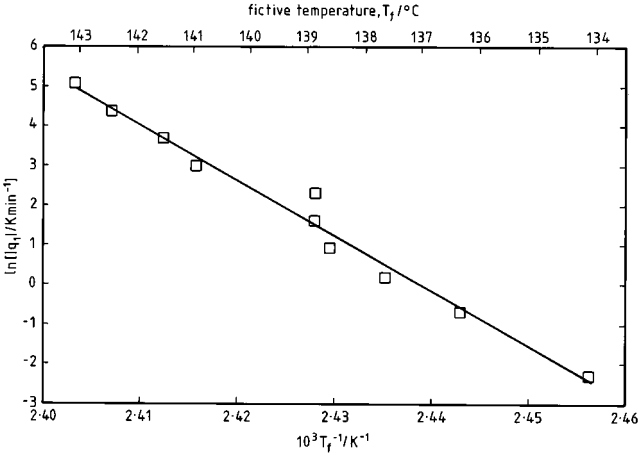

Figure 9. Plot of log(cooling rate) vs reciprocal fictive temperature for the cooling curves shown in Figure 8. The full line represents the least-squares fit to the data. The (nonlinear) scale along the top gives the values of the fictive temperature itself, for convenience.

eq 3, making use of the preceding calculation. This gives $\hat{s}(D) = 0.99$, and hence from the master curve in Figure 3 one obtains $x = 0.46 \pm 0.02$.

The heating scans for samples cooled at different rates and then immediately reheated are shown in Figure 8. The fictive temperature T_f for each cooling rate was found by the equal areas method,[11] and the results are plotted as log(cooling rate) vs reciprocal fictive temperature in Figure 9. A reasonable straight line can be fit to the data (correlation coefficient = 0.980) which yields, from the slope, $\Delta h^*/R = 140$ kK and hence an apparent activation energy of $\Delta h^* = 1160$ kJ mol^{-1}.

It is clear from the heating curves shown in Figure 8 that the peak temperature initially decreases as the cooling rate decreases and then, when the cooling rate decreases below about 2.5 K min^{-1}, it begins to increase

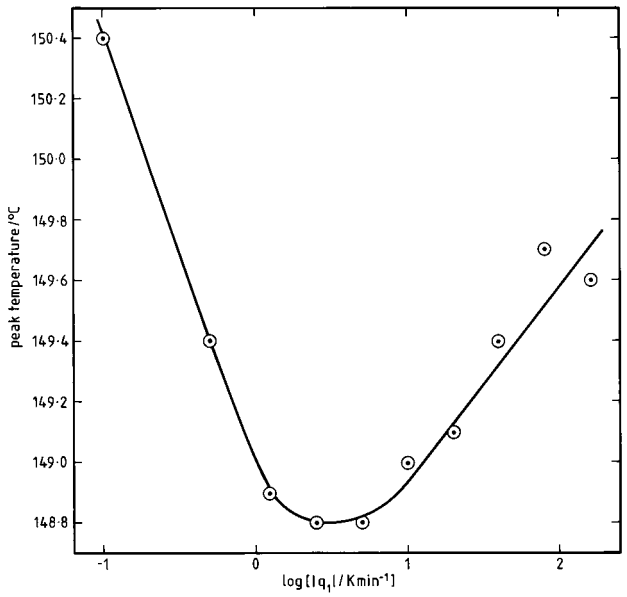

Figure 10. Dependence of peak temperature on log(cooling rate) for the heating curves shown in Figure 8.

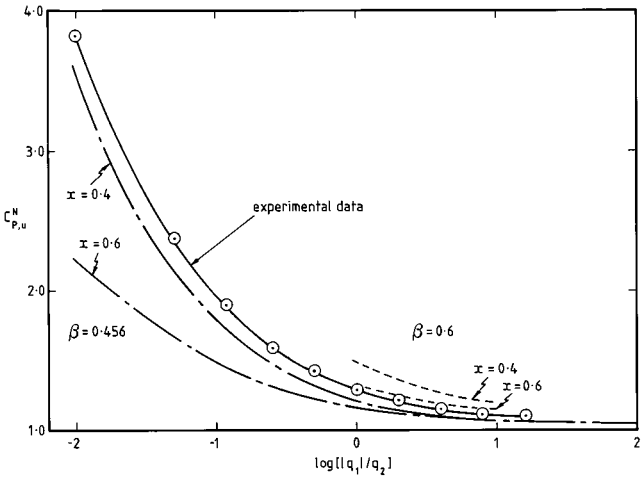

Figure 11. Normalized upper peak height $C_{p,u}^N$ plotted as a function of log(cooling rate/heating rate) for polycarbonate, evaluated from the heating curves in Figure 8. The experimental data are shown as open circles and are joined by a full line. Theoretical results are also given for a number of combinations of β and x: $\beta = 0.6$ shown by the dashed line, with $x = 0.4$ and $x = 0.6$ as indicated; $\beta = 0.456$ shown by the dash−dotted line, again for $x = 0.4$ and $x = 0.6$ as indicated.

again (see Figure 10). This behavior is anticipated[12,20] and represents a change in the nature of the endothermic peak from an upper peak (invariant with annealing time) at the faster cooling rates, which gives poorly stabilized glasses with large values of excess enthalpy before reheating, to a main or annealing peak (strongly dependent on annealing time) at the slower cooling rates, which give increasingly well stabilized glasses with reduced values of excess enthalpy before reheating.

The data shown in Figure 8 may also be used in the estimation of the nonexponentiality parameter β. The normalized upper peak height, $C_{p,u}^N$, is calculated from these curves in the manner described in the preceding section 3.1, and is plotted as a function of the logarithm of the ratio of cooling rate to heating rate in Figure 11. Included in this figure are theoretical results obtained using the equations for relaxation kinetics described

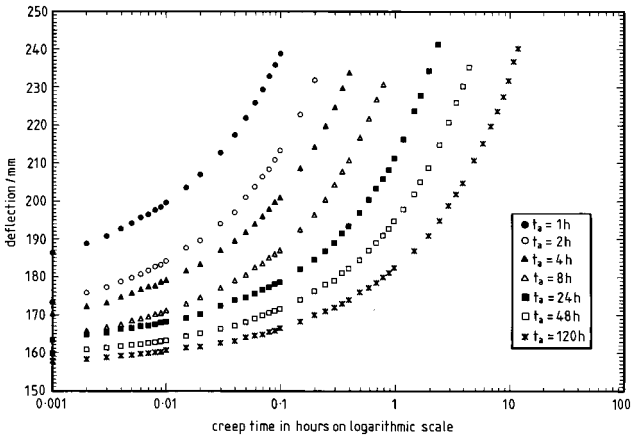

Figure 12. Creep of polycarbonate at 125 °C following a quench from 160 °C and then aging at 125 °C for the times indicated by the symbols. Note that the duration of each creep curve is one-tenth of the relevant aging time.

earlier, incorporating in particular the two parameters β and x. The theoretical curves are obtained from calculations made using certain discrete values of β and x, and also discrete values of cooling and heating rates; consequently this approach only allows one to estimate β within certain limits.

With the values of $x = 0.46 \pm 0.02$ obtained above by the peak shift method, independent of any assumptions about β, it can be seen that the experimental data in Figure 11 lie between the theoretical curves that would obtain (by interpolation) with $\beta = 0.456$ and $\beta = 0.6$, together with this value of $x = 0.46$. Thus we can estimate that β for enthalpy relaxation in this polycarbonate sample lies in the range $0.456 < \beta < 0.6$.

It may be useful at this point to summarize the important experimental parameter values that have been obtained, as follows:

$$\left(\frac{\partial T_p}{\partial(\log[t_a])}\right)_{q_1,T_a,q_2} = 2.58 \text{ K per decade}$$

$$\left(\frac{\partial \bar{\delta}_H}{\partial(\log[t_a])}\right)_{q_1,T_a,q_2} = 0.67 \text{ J g}^{-1} \text{ per decade}$$

$$\Delta C_p = 0.258 \pm 0.006 \text{ J g}^{-1} \text{ K}^{-1}$$

$$x = 0.46 \pm 0.02$$

$$\Delta h^* = 1160 \text{ kJ mol}^{-1} \; [\Delta h^*/R = 140 \text{ kK}]$$

$$0.456 < \beta < 0.6$$

4.2. Creep Response. The creep data for the polycarbonate sample quenched from 160 to 125 °C and then aged at 125 °C for times up to 120 h are shown in Figure 12 as deflection vs log(creep time). Superposition by means of horizontal shifting alone is unable to produce a satisfactory master curve. Each curve clearly has a different slope at any value of deflection, and the result is that the individual curves cross over each other rather than superpose. The immediate implication of this is that aging affects the values of the limiting compliances, J_U and J_R.

Accordingly, both horizontal and vertical shifts were used to superpose the creep curves, and the resulting master curve shows excellent superposition over the full

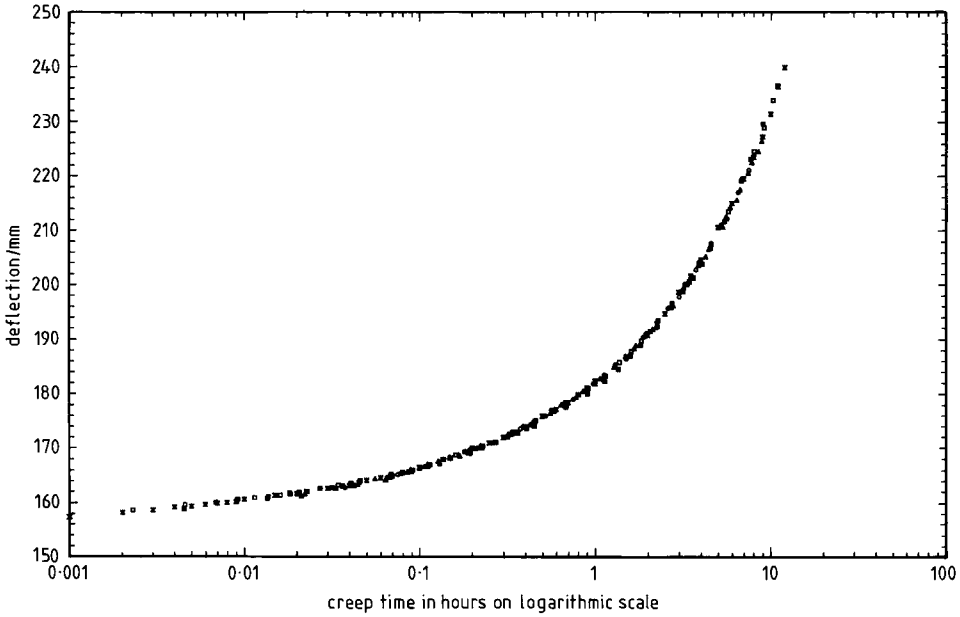

Figure 13. Master curve obtained by horizontal and vertical shifting of the creep curves in Figure 12. The reference curve was taken to be that for an aging time of 120 h, and the other curves were shifted to superpose. The symbols are the same as those in Figure 12 representing the different aging times.

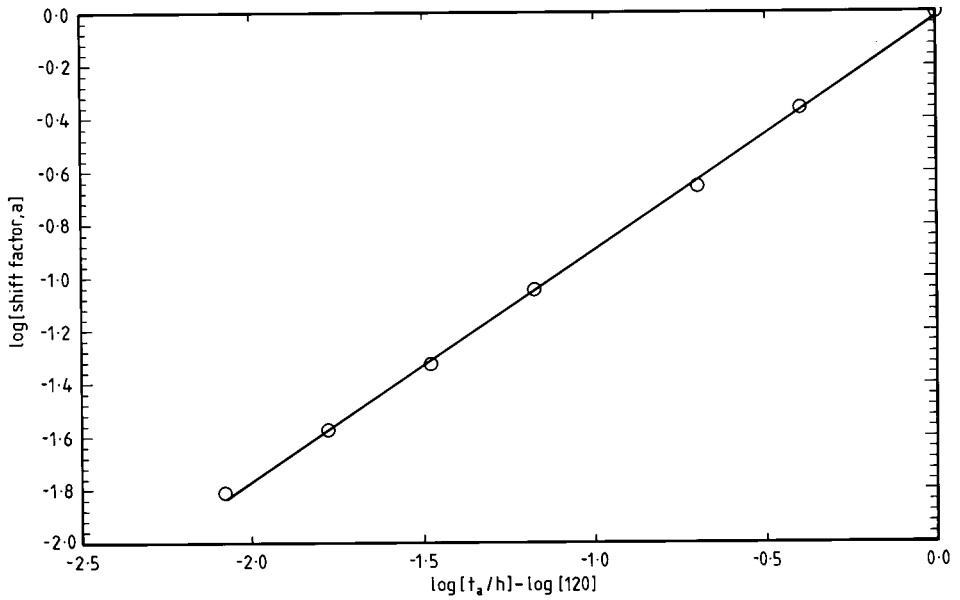

Figure 14. Log (horizontal shift factor) vs log(t_a/120) for the horizontal shift factors used to obtain the master curve of Figure 13 by superposing the creep curves of Figure 12. The reference aging time is 120 h. The line is a least-squares fit with a correlation coefficient of 0.999.

range of 4 decades, as can be seen in Figure 13. The reference curve was taken to be that for the longest aging time, $t_a = 120$ h, and the horizontal shift factor a is plotted against the aging time, relative to the reference aging time, on a log−log plot in Figure 14. Using the definition of Struik,[1] the shift rate at 125 °C for polycarbonate is found from the slope of the best fit straight line in Figure 14 to be $\mu = 0.87$.

The vertical shifts were measured directly in units of deflection (i.e. millimeters), and show a rather consistent trend with aging time as can be seen in Figure 15. The direct shift, rather than the shift factor was used here because in order to determine the latter it is necessary to make reference to the value of the unrelaxed compliance, J_U. It can be seen clearly from the master curve in Figure 13, however, that even at the shortest creep times for the longest aging time the unrelaxed portion of the relaxation is not well defined. In any case, the purpose of illustrating the vertical shift in Figure 15 is to show that there is a consistent behavior on aging rather than to extract a quantitative analysis.

The assumption made in superposing the creep curves by means of both horizontal and vertical shifts is that the relaxation strength remains constant. There is no need to make this assumption if, as explained in an earlier section, the creep rate vs creep time curves are superposed on a log−log plot by means of both horizontal and vertical shifts. The original creep data (deflection vs linear time) were differentiated by numerical differences and a quadratic smoothing routine. Because small differences are involved, a significant amount of scatter is introduced into the creep rate values, and hence the superposition process becomes more inexact than for the

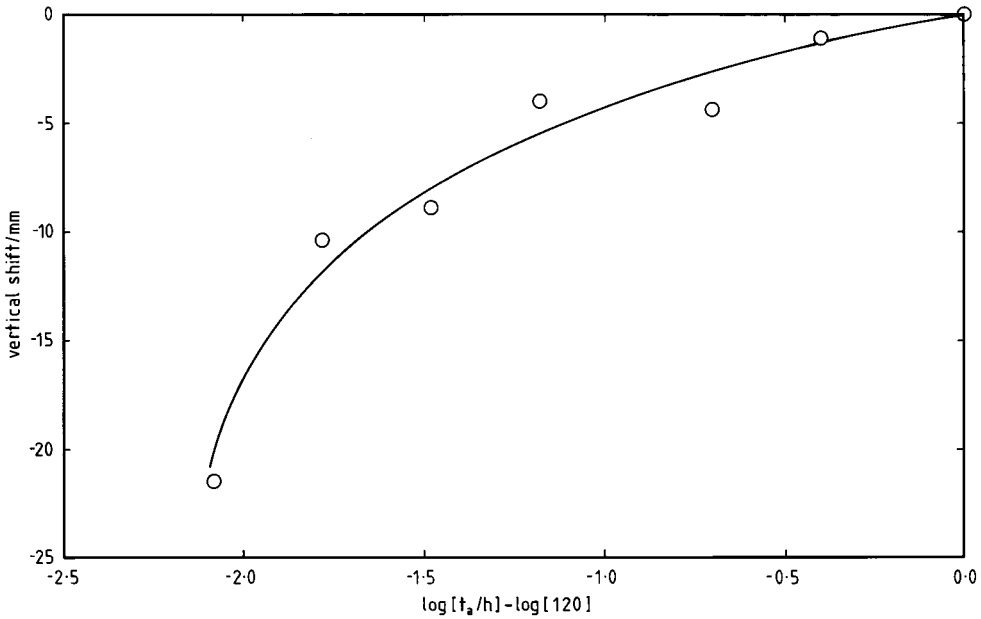

Figure 15. Vertical shifts (in units of millimeters) of the creep data in Figure 12 used to obtain by superposition the master curve shown in Figure 13. The reference aging time is $t_a = 120$ h.

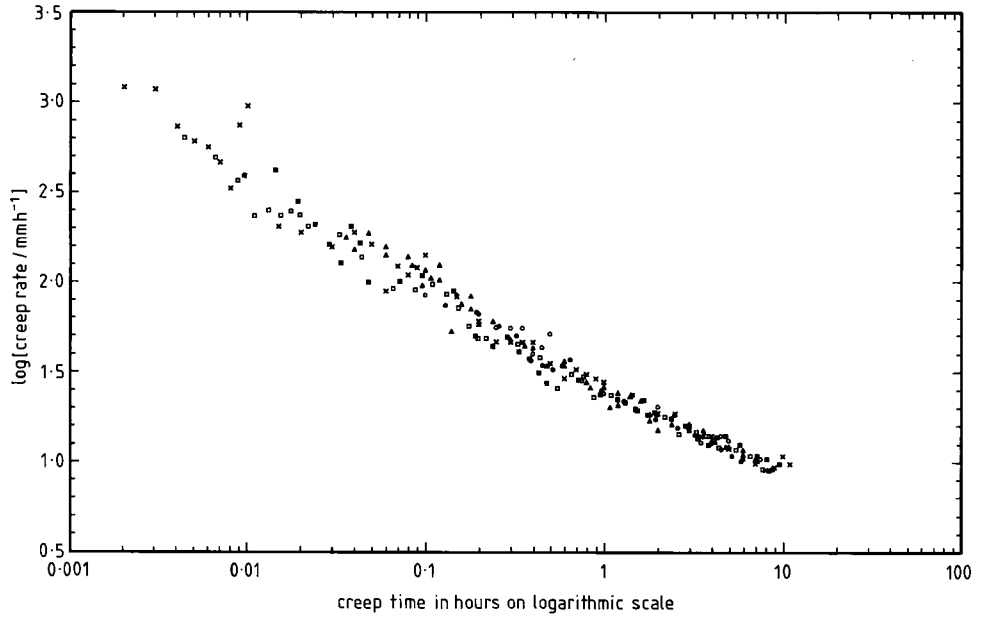

Figure 16. Master curve for the superposition of log(creep rate) vs log(creep time) derived from the original creep data of Figure 12. The reference aging time is $t_a = 120$ h, and the other curves are shifted onto this. The symbols representing the different aging times are given in Figure 12.

superposition of the original data. This can be seen in the master curve shown in Figure 16 for the superposition of the log(creep rate) vs log(creep time) data. Both horizontal and vertical shifts were used here, the former giving log a and the latter log a − log b, where the shift factor b relates to changes in relaxation strength. Within the limits imposed by the uncertainty in the values of the creep rate, as explained above, the optimum superposition of the log(creep rate) data was found to occur for $b = 1$, i.e., for log $b = 0$, which implies a shift of the data parallel to a line with a 45° slope. Since this approach then reduces to become equivalent to the horizontal plus vertical shifting procedure adopted immediately above in achieving the master curve of Figure 13, the same shift factor a and shift rate μ should be obtained. The shift factors a used to produce the master curve of Figure 16 are shown on a log−log plot in Figure 17 from which a shift rate of $\mu = 0.90$ is obtained. Given the extensive treatment of the data required in this analysis, this is in good agreement with the value of $\mu = 0.87$ obtained immediately above.

4.3. Tensile Tests. The nominal stress vs nominal strain curves were obtained for the polycarbonate samples annealed for various times at 125 °C and tested at room temperature at a cross-head speed of 2 mm min^{-1}, similar to the curves shown in Figure 4. From these curves, the yield stress and drawing stress were evaluated and are plotted as a function of log(aging time) in Figure 18. It can be seen that there is a significant increase in the yield stress, by 20% or so over approximately 3 decades of aging time, with no indication of any approach to equilibrium. On the other hand, the drawing stress shows a much smaller increase, barely more than 5% over the same 3 decade interval

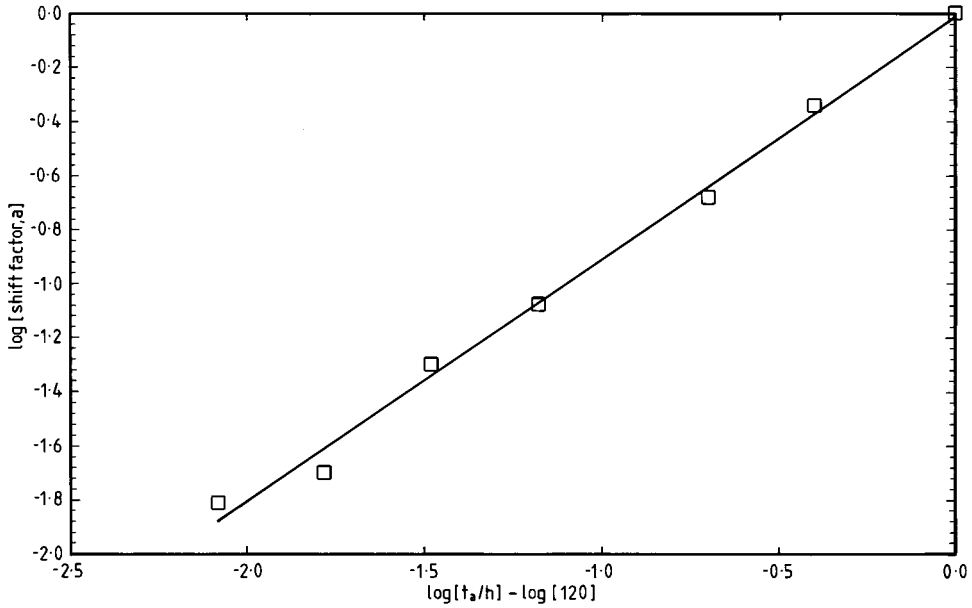

Figure 17. Horizontal shift factors used to superpose the log(creep rate) data of Figure 16, plotted as log(shift factor) vs log(creep time) relative to the reference aging time of $t_a = 120$ h. The line is a least-squares fit with a correlation coefficient of 0.994.

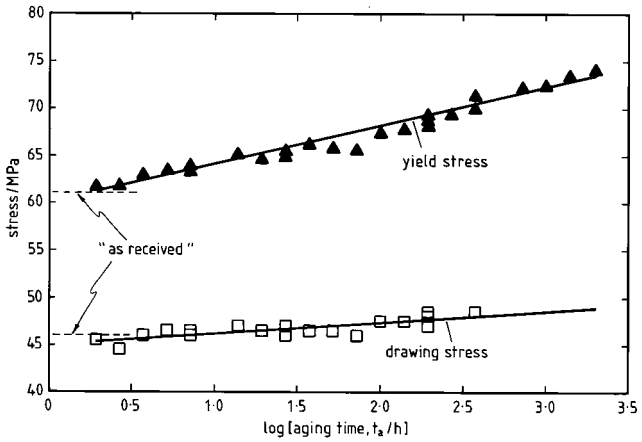

Figure 18. Yield stress (filled triangles) and drawing stress (open squares) as a function of log(aging time) for polycarbonate annealed at 125 °C. The "as-received" values, indicated by dashed lines, were obtained for samples machined from the extruded sheet and tested without any thermal pretreatment. The straight lines are least-squares fits to the data.

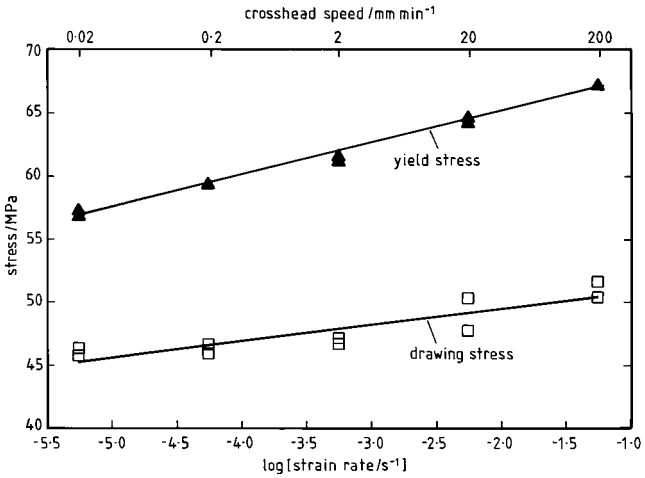

Figure 19. Dependence of the yield stress (filled triangles) and of the drawing stress (open squares) on log(strain rate) for tensile tests on "as received" polycarbonate samples at room temperature. For convenience, the cross-head speed is also given on the uppermost scale. The straight lines represent least-squares fits to the data.

of aging time. It can also be seen that there is only one data point for the drawing stress for aging times greater than 200 h; the reason for this is that, in parallel with the increase in yield stress, there is a reduction in the strain as the material loses ductility, such that for aging times longer than 200 h the samples fail (except in a single case) soon after yield and do not reach the drawing stage. The slopes of the best fit lines gives $d\sigma_y/d(\log t_a) = 4.07$ MPa per decade for the yield stress σ_y, with a correlation coefficient of 0.962, and $d\sigma_d/d(\log t_a) = 1.17$ MPa per decade for the drawing stress σ_d, with a correlation coefficient of 0.674.

The strain dependence of the yield and drawing stresses was also determined, for the "as received" samples, over four decades of strain rate. The results are shown in Figure 19. Similar to the results for the effect of aging time, the yield stress increases with log (strain rate) at a significantly greater rate than does the drawing stress. The slopes of the best fit straight lines give $d\sigma_y/d(\log \dot{\epsilon}) = 2.53$ MPa per decade for the yield stress, with a correlation coefficient of 0.993, and $d\sigma_d/d(\log \dot{\epsilon}) = 1.27$ MPa per decade for the drawing stress, with a correlation coefficient of 0.791.

5. Discussion

In view of the rather wide scope of this paper, it will be convenient to discuss the results under separate headings.

5.1. Enthalpy Relaxation Parameters. The parameters describing the kinetics of enthalpy relaxation (x, Δh^*, β) of polycarbonate have been evaluated here by the peak shift method, and have been summarized above. The same parameters have previously been determined by Hodge[26] by the curve fitting method, with the following results: $x = 0.19$, $\Delta h^* = 1250$ kJ mol^{-1} [$\Delta h^*/R = 150$ kK], and $\beta = 0.46$. It is clear that there is good agreement between the values for the apparent activation energy, and reasonable agreement in respect of the value of β, although that from the peak shift method ($0.456 < \beta < 0.6$) is likely (in view of the

location of the experimental data with respect to the theoretical curves in Figure 11) to be slightly greater than the value of 0.46 found by curve fitting. There is, however, a large discrepancy between the values obtained by the two methods for the nonlinearity parameter x, the reason for which needs to be considered.

First of all, it should be noted that the curve fitting parameters given above differ slightly from the original values.[27] In the original work,[27] the curve fitting procedure gave $x = 0.22$ and $\beta = 0.54$, each with an uncertainty of ± 0.05, and $\Delta h^*/R = 150 \pm 15$ kK. In the later work,[26] which introduced improved numerical analysis procedures, the slightly different values of $x = 0.19$ and $\beta = 0.46$, with the same value for $\Delta h^*/R$, are quoted. However, if the same uncertainty exists for these latter values as for the original ones (i.e. ± 0.05 for both x and β), then there is no significant difference introduced by the improved analysis. This leaves the discrepancy between our value of $x = 0.46$ and Hodge's value of $x = 0.19$, however, which is a much greater difference than would be accounted for even if the uncertainties in each were ± 0.05.

A second point to consider in trying to resolve this discrepancy is to examine the range of experimental data covered by the original data in order to permit these parameter values to be found. In Hodge's work,[27] three types of experiment were performed: (i) cooling rate experiments, with rates varied between 5 and 40 K min^{-1} and with no annealing; (ii) annealing experiments with a fixed annealing time of 1 h at annealing temperatures about 10, 20, and 30 K below T_g; (iii) annealing experiments involving annealing times from 1 to about 26 h at an annealing temperature about 30 K below T_g. The point of interest here is the amount of annealing that can take place during these latter two types of experiment. Recalling that the parameter x describes the nonlinearity of the kinetics, it will have a more pronounced effect on the response the further the system is displaced from equilibrium. One simple measure of this displacement from equilibrium is the magnitude of the overshoot in C_p, or its value C_p^N when normalized to ΔC_p.

For Hodge's experiments of type i, for which the curves are available in Figure 8 of ref 26 or in Figure 5 of ref 27, the C_p^N (in fact these are upper peaks, and hence $C_{p,u}^N$ values; cf. eq 5) values range from 1.2 to 1.6. This is seen to be a very small variation when compared with the range of values covered in the present work, shown in Figure 11. Furthermore, in the present work these experiments are not used in the evaluation of x, since they lead mainly to upper peaks, which are insensitive to annealing. An examination of Figure 10 shows that, for heating scans at 10 K min^{-1}, as is used in Hodge's work, cooling rates greater than 5 K min^{-1} lead to upper peaks (the part of this curve with a positive slope), whereas it is only with cooling rates somewhat less than 2.5 K min^{-1} that the main annealing peaks appear (the part of this curve which has a negative slope). It seems, therefore, that Hodge's experiments of type i are not a good basis for the evaluation of x, since there will be only a very limited effect of nonlinearity.

For the experiments of types ii and iii, Hodge's data can be found in Figures 9 and 10 of ref 26 and in Figure 6 of ref 27. In these annealing experiments, the maximum C_p^N values are about 3.2 and 3.4, respectively. Compare this with the maximum value of about 8.3 which may be estimated from the curves in Figure 5, and it can be seen that the present work covers a wider range of structural states, involving considerably greater degrees of nonlinearity, and hence provides a better basis for the evaluation of the nonlinearity parameter. Indeed, this can further be seen from Figure 6, where for an aging time of 1 h it is upper peaks rather than annealing peaks which appear. Hodge's experiments of type ii, which involve an annealing time of only 1 h, do not therefore provide the optimum data for the evaluation of the nonlinearity parameter, at least for annealing temperatures of 20 and 30 K below T_g.

In summary on this particular aspect, we believe that Hodge's experiments are not well designed for the evaluation of the parameter x since they do not, on the whole, involve sufficiently large departures from equilibrium on heating, and hence do not introduce sufficient nonlinearity. The thermal history that Hodge found most difficult to fit was the 16 h anneal at $T_g - 30$ K, which was the one giving the largest overshoot ($C_p^N = 3.4$), yet even this is less than half of the maximum C_p^N value shown in the present work. The fit to this particular set of data (Figure 10 in ref 26) shows that the theoretical curve significantly overestimated the C_p^N value at the peak and gives too narrow a peak; both of these features are characteristic of too small a value for x.[17] We therefore consider the value of $x = 0.46 \pm 0.02$ to be more reliable. (See note added in proof.)

5.2. Comparison of Enthalpy Relaxation and Creep. It has been shown that the physical aging of the creep curves for polycarbonate at 125 °C can be characterized by a shift rate $\mu = 0.87$. This value is typical for the aging behavior of nearly all amorphous polymers,[1] for which μ is close to unity over a more or less wide range of temperature below T_g. This physical aging behavior is commonly believed to be linked to the structural changes taking place in the material, which may themselves be characterized by the enthalpy relaxation measurements. It is therefore of considerable interest to compare the time scales and rates of physical aging as it is manifest by creep and enthalpy measurements.

We have considered that enthalpy relaxation can be described using the TNM eq 1, which relates the (single) relaxation time to the temperature T and to the structure, determined by the fictive temperature T_f. For the more realistic situation of a distribution of relaxation times, the usual assumption (also made here) is that each element of the discrete distribution depends in the same way on the fictive temperature, thus ensuring thermorheological simplicity. Likewise, in the case of a continuous spectrum simulated by the stretched exponential response function of (2), the characteristic time τ also has the same dependence on T_f. Thus in all cases one can describe the isothermal change in the relaxation time with structure during aging by

$$\ln \tau = A + \frac{(1 - x)\Delta h^*}{RT_f} \tag{9}$$

where $A = \ln \tau_o + x\Delta h^*/RT$ is a constant at a given isothermal temperature.

Differentiating this with respect to T_f, one obtains

$$\frac{d(\ln \tau)}{dT_f} = -\frac{(1 - x)\Delta h^*}{RT_f^2} = -(1 - x)\theta \tag{10}$$

where $\theta = \Delta h^*/RT_f^2$ is a parameter introduced in the

KAHR model,[12] and is found as 0.80 K^{-1} for $\Delta h^*/R$ = 140 kK and T_f = 418 K (145 °C).

The definition of T_f allows one to write the following relationship between T_f and $\bar{\delta}_H$, the enthalpy lost during annealing

$$\frac{dT_f}{d\bar{\delta}_H} = -\frac{1}{\Delta C_p} \tag{11}$$

so that (10) can then be rewritten as

$$\frac{d(\ln \tau)}{d\bar{\delta}_H} = (1-x)\theta/\Delta C_p \tag{12}$$

The same equation can be written directly from the equivalent expression to the TNM equation as used in the KAHR model.[12]

Finally, the dependence of the enthalpy relaxation time on the aging time t_a can be found as

$$\mu_H = \frac{d(\ln \tau)}{d(\ln t_a)} = \frac{(1-x)\theta}{2.303\Delta C_p}\left(\frac{d\bar{\delta}_H}{d(\log t_a)}\right) \tag{13}$$

where $d\bar{\delta}_H/d(\log t_a)$ is the slope of the plot of enthalpy loss as a function of log(aging time), shown earlier in Figure 7. The use of μ_H in (13) indicates that this is an "enthalpy shift rate", in analogy with the shift rate μ used for the mechanical response.

This relationship between enthalpy relaxation time and aging time can be evaluated quite simply from (13) since all the parameters have been determined above in the analysis of the enthalpy relaxation experiments. Substituting in the appropriate values gives $\mu_H = 0.49$. The difference between this value for enthalpy relaxation and the shift rate $\mu = 0.87$ for aging of the creep response is very significant. It implies that the mechanical relaxation time spectrum, or its characteristic relaxation time, is not linearly related to the equivalent spectrum or characteristic relaxation time for enthalpy relaxation. The relative magnitudes of the two shift rates suggests that the aging of the mechanical response occurs considerably more rapidly than does enthalpy relaxation. (See note added in proof.)

We note that a comparison of the relaxation rates μ_H and μ does not imply a comparison of the time scales required for the attainment of equilibrium. The aging temperature about 20 K below T_g was selected for the enthalpy relaxation experiments deliberately so that the "limiting conditions" required for the evaluation of x by the peak shift method could be achieved.[17,18] At this aging temperature, both the peak endotherm temperature and the enthalpy loss (Figures 6 and 7) continue to increase with aging time beyond 2000 h, so that attainment of equilibrium is impossible within experimental time scales. Thus these experiments cannot provide information about the relative time scales for attaining equilibrium by the different measuring techniques, which would instead require an aging temperature much closer to the nominal T_g of 145 °C.

A similar "volumetric shift rate" may be defined as

$$\mu_V = \frac{(1-x)\theta}{2.303\Delta\alpha}\left(\frac{d\bar{\delta}}{d(\log t_a)}\right) \tag{14}$$

where $\bar{\delta}$ is the change in δ that occurs on aging, δ being the relative departure of the volume (v) from its equilibrium value (v_∞) at the same temperature, $\delta = (v - v_\infty)/v_\infty$, and $\Delta\alpha$ is the difference between the thermal expansion coefficients of the liquid and glass. Assuming that the same value of x pertains for both enthalpy and volume relaxation (as has been observed before for polystyrene[28]), taking $\Delta\alpha = 2.81 \times 10^{-4}$ K^{-1},[29] assuming $\theta = 0.80$ K^{-1} as for enthalpy relaxation, and using the value of 8.4×10^{-4} for the change of $\bar{\delta}$ with log(aging time), being an average of 8.5×10^{-4} from ref 30 and 8.3×10^{-4} from ref 31, one obtains $\mu_V = 0.56$. Thus the relative magnitudes of these shift rates are $\mu > \mu_V > \mu_H$, and this could provide a means of comparing the relaxation rates during physical aging for each of these experimental measurements. A similar approach was adopted by Málek and Montserrat,[32] who defined normalized relaxation rates by dividing the simple isothermal enthalpic and volumetric relaxation rates by ΔC_p and $\Delta\alpha$, respectively. The difference between these normalized relaxation rates and the shift rates μ_H and μ_V defined here lies in the $(1-x)\theta$ term included in the latter. Interestingly, the relative magnitudes of μ, μ_V, and μ_H found here for polycarbonate correspond to the relative time scales for mechanical, volumetric, and enthalpic relaxation in poly(methyl methacrylate) determined by Perez et al.,[33] which increase in the same order.

It is worth noting, however, that there could be a certain inconsistency in this approach to defining relaxation rates. In the limiting (and unrealistic) case where there is no nonlinearity in the relaxation, hence $x = 1$, the above definitions of the shift rates for enthalpy and volume would imply $\mu_H = 0$ and $\mu_V = 0$. Under these circumstances, the relaxation time is constant and the enthalpy and volume recovery would both be exponential for a single relaxation time or would be defined by a stretched exponential decay for a spectrum. Instead of comparing the relaxation times for mechanical, enthalpic and volumetric relaxation, therefore, it may be preferred to examine directly the relationship between the mechanical relaxation time, τ_c in (8), and (in the present instance) the enthalpy loss, $\bar{\delta}_H$.

If τ_c were linearly dependent on $\bar{\delta}_H$, then the linear dependence of log a on log t_a for the mechanical creep response would imply a similar linear dependence of log $\bar{\delta}_H$ on log t_a. Instead, though, it is $\bar{\delta}_H$ which is linearly dependent on log t_a (see Figure 7). The implication of this would be that τ_c depends exponentially rather than linearly on $\bar{\delta}_H$. This conclusion would be somewhat speculative, but serves to highlight the problems surrounding the continued debate on the relationship between the aging responses monitored by different techniques such as enthalpy relaxation, volume relaxation and mechanical response (see for example the discussion in ref 5). Unfortunately, for the aging temperature of 125 °C used here, it was not possible to achieve equilibrium within the experimental time scale of about 2000 h with either of the techniques (creep, enthalpy), and therefore the relative time scales for the achievement of equilibrium could not be determined.

A further point is also worth noting. The shift rate μ for the creep response was found by means of both horizontal and vertical shifting of the creep data in Figure 12. An excellent master curve (Figure 13) was obtained in this way, which gave consistent vertical shifts (Figure 15) and was consistent also with the shifts obtained by superposing the creep rates on a log−log plot (Figure 17), a method originally proposed by Chai

and McCrum.[21] It is interesting to observe for the log(creep rate) data in Figure 16 that there is a small upward curvature rather than the downward curvature that would be anticipated for a unimodal distribution of creep relaxation times.[21] This upward curvature has, in fact, now been observed in this kind of analysis for other linear polymers, namely polystyrene and polypropylene,[7,34,35] and also for a fully cross-linked epoxy-anhydride resin.[36]

5.3. Alternative Formalisms to TNM. The theoretical approach introduced in section 3.1 and utilized in section 5.2 for the evaluation of an enthalpy shift rate was based upon the TNM equation. The reason for this was stated briefly earlier, but it would be interesting to examine to what extent our conclusions might be modified if we were instead to make use of an alternative formalism, and in particular that due to Adam and Gibbs.[14]

Two of the criticisms often leveled at the TNM equation are (i) that it implies an Arrhenius temperature dependence for the relaxation time(s) in equilibrium, whereas it is known that most polymers are rather "fragile", in Angell's terminology,[37] and hence display a marked curvature in a plot of log τ vs reciprocal temperature,[38] and (ii) that the physical significance of the nonlinearity parameter x is questionable. The Adam−Gibbs (AG) approach supposedly overcomes these objections. It is based upon the original analysis of Adam and Gibbs[14] who considered the configurational entropy S_c of cooperatively rearranging regions in order to derive an expression for the temperature dependence of the relaxation time in equilibrium:

$$\tau = A \exp\left[\frac{N_A s_c^* \Delta\mu}{kTS_c}\right] \tag{15}$$

Here A is a constant, N_A is Avogadro's number, s_c^* is the configurational entropy of the smallest cooperatively rearranging region that permits a transition from one configuration to another, $\Delta\mu$ is the potential energy hindering the cooperative rearrangement per monomer segment, and k is Boltzmann's constant. The configurational entropy may be evaluated from

$$S_c = \int_{T_2}^{T} \frac{\Delta C_p}{T}\, dT \tag{16}$$

where T_2 is the Kauzmann temperature at which the configurational entropy is zero. Hodge[2] identifies two possibilities for the temperature dependence of ΔC_p, namely $\Delta C_p = CT_2/T$, the hyperbolic form where C is the value of ΔC_p at $T = T_2$, and ΔC_p = constant = C. These two dependences yield two forms for $S_c(T)$:

$$S_c(T) = C\left(1 - \frac{T_2}{T}\right) \tag{17}$$

the so-called AGV (for "Vogel−Tammann−Fulcher" or VTF) form, and

$$S_c(T) = C \ln\left(\frac{T}{T_2}\right) \tag{18}$$

the so-called AGL (for "logarithmic") form, respectively. The former yields the VTF equation, characteristic of the temperature dependence of the relaxation time for fragile systems.

In the AG formalism, the usual way in which nonlinearity is introduced is by assigning to S_c an entirely fictive temperature dependence,[2] eliminating any dependence on the actual temperature. Thus (15) becomes

$$\tau(T,T_f) = A \exp\left[\frac{N_A s_c^* \Delta\mu}{kTS_c(T_f)}\right] \tag{19}$$

where

$$S_c(T_f) = C\left(1 - \frac{T_2}{T_f}\right) \tag{20}$$

for AGV, and

$$S_c(T_f) = C \ln\left(\frac{T_f}{T_2}\right) \tag{21}$$

for AGL.

Comparison of the parameter values from the two approaches, TNM and AG, may be made by considering a narrow temperature interval and examining the dependence of τ on both T and T_f. Thus Hodge[2] has shown that

$$x \approx 1 - \frac{T_2}{T_f} \tag{22}$$

and

$$\frac{N_A s_c^* \Delta\mu}{kC} = Q \approx x^2 \frac{\Delta h^*}{R} \tag{23}$$

for AGV. Similarly, it can be shown that

$$\frac{x}{1-x} \approx \ln\left(\frac{T_f}{T_2}\right) \tag{24}$$

and

$$Q \approx \frac{x^2}{1-x} \frac{\Delta h^*}{R} \tag{25}$$

for AGL. The validity of the assumption of a narrow temperature interval is supported by the curve-fitting analysis of Hodge[26] for a variety of glassy polymers, for which he finds the TNM values for the nonlinearity parameter x to be very close to the equivalent values of x obtained using AGV and AGL together with (22) and (24), respectively.

Following the procedure adopted in section 5.2 above, we can therefore evaluate enthalpy shift rates according to AGV and AGL, by finding the isothermal fictive temperature dependence of τ by differentiating (19)

$$\frac{d(\ln \tau)}{dT_f} = -\frac{Q}{T\left[1 - \frac{T_2}{T_f}\right]^2} \frac{T_2}{T_f^2} \tag{26}$$

for AGV, and

$$\frac{d(\ln \tau)}{dT_f} = -\frac{Q}{T\left[\ln\left(\frac{T_f}{T_2}\right)\right]^2} \frac{1}{T_f} \tag{27}$$

for AGL.

Likewise, we have $dT_f/d\bar{\delta}_H = -T_f/CT_2$ for AGV and $dT_f/d\bar{\delta}_H = -1/C$ for AGL, and hence

$$\frac{d(\ln \tau)}{d\bar{\delta}_H} = \frac{Q}{CTT_f\left(1 - \frac{T_2}{T_f}\right)^2} \tag{28}$$

for AGV, and

$$\frac{d(\ln \tau)}{d\bar{\delta}_H} = \frac{Q}{CTT_f\left[\ln\left(\frac{T_f}{T_2}\right)\right]^2} \tag{29}$$

for AGL.

Finally, making use of the parameter correlations in (22) to (25) together with the definitions of $C = \Delta C_p T_f/T_2$ for AGV and $C = \Delta C_p$ for AGL, both evaluated at T_f, we find

$$\frac{d(\ln \tau)}{d\bar{\delta}_H} = \frac{(1-x)}{\Delta C_p}\frac{\Delta h^*}{RTT_f} \tag{30}$$

for both AGV and AGL, which is identical to (12), derived from the TNM equation, when evaluated at $T = T_f$ and when the relationship between θ and Δh^* is noted. Hence we may conclude that the expression for the enthalpy shift rate μ_H given by (13) is independent of the approach, TNM or AG, used in its derivation.

We emphasize that this conclusion is based upon the assumption that we are considering a narrow temperature interval around T_g. Support for this assumption was mentioned above in respect of Hodge's parameter values derived by the two different approaches.[26] Further support may also be gained from remarking that the dependence of the reciprocal of the fictive temperature on the log(cooling rate), illustrated in Figure 9, is essentially linear. In other words, over the temperature range covered by the fictive temperature in these experiments, the Arrhenius equation is an acceptable approximation.

Despite the advantage that AG offers over TNM in that it has greater physical significance, we believe nevertheless that its nonlinear formalism is not wholly appropriate. The AGV and AGL expressions relating x and T_2, (22) and (24), respectively, allow a determination of T_2 for polycarbonate based upon our TNM value of $x = 0.46 \pm 0.02$ and assuming $T_f = T_g = 418$ K. Thus we find $T_2 \approx 226 \pm 8$ K for AGV and $T_2 \approx 178 \pm 13$ K for AGL, approximately 190 and 240 K, respectively, below T_g. These temperature differences are much greater than, for example, the "universal" WLF value of $T_g - T = 51.6$ K for the temperature interval below T_g at which the viscosity becomes infinite. Similarly large discrepancies have been noted for other polymers, particularly polystyrene.[2,39] The reason for this could lie in attributing to S_c in (20) and (21) only a fictive temperature dependence and not any actual temperature dependence. In our view, this automatically overemphasizes the nonlinearity in (19) where the temperature and structure dependence of τ are defined. Consequently, when attempting to fit either AGV or AGL to experimental data, the parameter value T_2, which may be associated with nonlinearity (higher values of T_2/T_f imply lower values of x and increased nonlinearity), will be underestimated in order to reduce the over-dependence of τ on T_f inherent in (19).

5.4. Yield Behavior. The first point to note from Figure 18 is the rather strong dependence of the yield stress, σ_y, of polycarbonate on the aging time, and its linear relationship with log t_a. This dependence has been known for a long time; for example, Golden et al.[40] reported the effect of thermal pretreatment on many properties of polycarbonate, including a significant increase of the yield stress on aging at a range of temperatures below T_g. Shortly thereafter, LeGrand[41] showed a linear increase in yield stress on annealing polycarbonate at 125 °C, and from these data (Figure 10 in ref 41) one can calculate $d\sigma_y/d(\log t_a) = 3.97$ MPa per decade, in excellent agreement with our results presented here.

More recently, Bauwens-Crowet and Bauwens[42] have also investigated the effect on the yield stress of polycarbonate of annealing below T_g. For an annealing temperature of 130 °C, they also find a linear relationship between σ_y and log t_a, over 3 decades of aging time (similar to the aging time range used in the present work), which gives a slope of $d\sigma_y/d(\log t_a) = 3.04$ MPa per decade. This value is rather smaller than those found by LeGrand[41] and in the present work; the reason for this may lie in the fact that Lexan polycarbonate (GE Plastics) was used in the work of LeGrand and in the present paper, whereas Bauwens-Crowet and Bauwens used Makrolon (Bayer) polycarbonate.

In addition to the yield stress dependence, Figure 18 also shows that the drawing stress is very much less influenced by the aging time. This, like the dependence of yield stress on aging time, has likewise been known for many years, though the literature data are not always wholly in agreement. For example, Adam et al.[43] report for polycarbonate (Makrolon, Bayer) an increase in both the yield stress and the "yield drop" with aging time, with the drawing stress still dependent on aging time, but to a lesser extent than the yield stress. On the other hand, Struik,[44] while also stating that the yield stress would be expected to depend on aging time much more than would the drawing stress, goes on to state that after yield the aging history will be erased and hence that the drawing stress should be independent of aging time.

The usual explanation for the difference between the effects of aging on the yield and drawing stresses is that rejuvenation (or "deaging") occurs on yielding. Thus in the experiments discussed here, the effect of aging is seen in the magnitude of the yield stress, but the process of yielding, which leads to the stress drop during the formation of the neck and which is the precursor of the drawing process, causes a certain amount of mechanical rejuvenation to occur. Hence much of the effect of aging is removed from the sample, and this is manifest as a drawing stress which is much less influenced by the aging time than is the yield stress.

It is also interesting to examine, from the results presented in Figure 19, the influence of the strain rate on the yield stress. There is a clear linear dependence of yield stress on log(strain rate), with a slope of 2.53 MPa per decade found for the effect of aging time. On the other hand, Bauwens-Crowet and Bauwens[42] find a slope of 3.03 MPa per decade for unannealed samples tested at room temperature, in respect of the dependence of σ_y on log(strain rate). The paradox here is that Bauwens-Crowet and Bauwens find the same dependence for the effects of both aging and strain rate on the yield stress, whereas our results presented here

indicate that these dependences are clearly different. Hence, in direct contrast to the conclusion reached by Bauwens-Crowet and Bauwens, we conclude from our results that the molecular time scale changes induced by the aging process are quite different from the effect of probing different molecular time scales by changing the strain rate. We believe that this is analogous to, and consistent with, our conclusion above that structural changes in the material that occur during aging, and which may be probed by for example enthalpy relaxation, do so on quite a different time scale from the changes in creep response that are presumed to result from these structural changes.

6. Conclusions

Three separate but interrelated sets of experiments have been performed to examine the effects of aging at 125 °C ($\approx T_g - 20$ K) on the behavior of polycarbonate, and the conclusions from each are summarized here.

Enthalpy relaxation has been studied by DSC, and the kinetic parameters describing the relaxation have been evaluated by the peak shift method. The values obtained are as follows: nonlinearity parameter $x = 0.46 \pm 0.02$; apparent activation energy $\Delta h^* = 1160$ kJ mol^{-1}, or $\Delta h^*/R = 140$ kK; nonexponentiality parameter β in the range $0.456 < \beta < 0.6$. The values for Δh^* and β are consistent with results presented earlier by Hodge, but there is a significant discrepancy in respect of the value of x. It is argued that the present result is more reliable. (See note added in proof.)

Creep experiments at low strain have been performed over a range of aging times, and it is shown that excellent superposition can be achieved by means of both horizontal and vertical shifts. The shift rate $\mu = 0.87$ is typical of glassy polymers just below T_g, but is shown to be significantly different from an equivalent "enthalpy shift factor" μ_H, which can be evaluated from the enthalpy relaxation data and gives $\mu_H = 0.49$. The implication of this is that the changes in enthalpy and in creep response during aging occur at quite different rates, and hence it is not possible to relate in a simple way the physical aging of the creep response and the structural changes identified by enthalpy loss. (See note added in proof.)

Tensile testing of annealed samples shows a linear increase of yield stress with log(aging time), as has been noted before, but the slope of this dependence is quite different from that of the similar linear increase of yield stress with log(strain rate). This is in direct contrast to earlier results of Bauwens-Crowet and Bauwens but is consistent with the conclusion above that different aging rates are observed when the aging process is probed by different techniques.

Note Added in Proof

The conclusion that μ and μ_H differ significantly is derived using theoretical considerations, based on either the TNM or AG expressions. It was usefully pointed out by one referee that, while this conclusion holds provided that these theoretical models are correct, the data may equally well, on the other hand, indicate that there is a serious problem with such models. In the latter case, the significance of the nonlinearity parameter x becomes questionable, and furthermore, its value may well depend upon the method of evaluation. In the present paper, we analyze tbe data using the current formalisms (TNM and AG), but we do not wish to exclude the possibility that these models are inadequate.

References and Notes

(1) Struik, L. C. E. *Physical Aging in Amorphous Polymers and Other Materials*; Elsevier: Amsterdam, 1978.
(2) Hodge, I. M. *J. Non-Cryst. Solids* **1994**, *169*, 211.
(3) Hutchinson, J. M. *Prog. Polym. Sci.* **1995**, *20*, 703.
(4) Hutchinson, J. M. Chapter 3 In *The Physics of Glassy Polymers*, 2nd ed.; Haward, R. N., Young, R. J., Eds.; Chapman and Hall: London, 1997; pp 85−153.
(5) Delin, M.; Rychwalski, R. W.; Kubat, J., Klason, C.; Hutchinson, J. M. *Polym. Eng. Sci.* **1996**, *36*, 2955.
(6) British Standard Methods of Testing Plastics, BS2782: Part 3: Method 320C: 1976. *Tensile strength, elongation and elastic modulus.*
(7) Kriesten, U. Ph.D. Thesis, University of Aberdeen, U.K., 1993.
(8) Kriesten, U.; Hutchinson, J. M. *Polymer* **1992**, *33*, 4875.
(9) Tool, A. Q. *J. Am. Ceram Soc.* **1946**, *29*, 240.
(10) Narayanaswamy, O. S. *J. Am. Ceram. Soc.* **1971**, *54*, 491.
(11) Moynihan, C. T.; Easteal, A. J.; DeBolt, M. A.; Tucker, J. *J. Am. Ceram. Soc.* **1976**, *59*, 12.
(12) Kovacs, A. J.; Aklonis, J. J.; Hutchinson, J. M., Ramos, A. R. *J. Polym. Sci., Polym. Phys. Ed.* **1979**, *17*, 1097.
(13) Kovacs, A. J.; Hutchinson, J. M.; Aklonis, J. J. In *The Structure of Non-Crystalline Solids*; Gaskell, P. H., Ed.; Taylor and Francis: London, 1977; p 153.
(14) Adam, G.; Gibbs, J. H. *J. Chem. Phys.* **1965**, *43*, 139.
(15) Scherer, G. W.*J. Am. Ceram. Soc.* **1984**, *67*, 504.
(16) Kovacs, A. J. *Fortschr. Hochpolym. Forsch.* **1963**, *3*, 394.
(17) Ramos, A. R.; Hutchinson, J. M.; Kovacs, A. J. *J. Polym. Sci., Polym. Phys. Ed.* **1984**, *22*, 1655.
(18) Hutchinson, J. M.; Ruddy, M. *J. Polym. Sci., Polym. Phys. Ed.* **1988**, *26*, 2341.
(19) Richardson, M. J.; Savill, N. G. *Polymer* **1975**, *16*, 753.
(20) Hutchinson, J. M.; Ruddy, M. *J. Polym. Sci., Polym. Phys. Ed.* **1990**, *28*, 2127.
(21) Chai, C. K.; McCrum, N. G. *Polymer* **1980**, *21*, 706.
(22) McCrum, N. G.; Read, B. E.; Williams, G. *Anelastic and Dielectric Effects in Polymer Solids*; Wiley: New York, 1967.
(23) Hutchinson, J. M. *Lect. Notes Phys.* **1987**, *277*, 172.
(24) Bauwens-Crowet, C., Bauwens, J. C. *Polymer* **1986**, *27*, 709.
(25) Cheng, T. W.; Keskkula, U.; Paul, D. R. *J. Appl. Polym. Sci.* **1992**, *45*, 531.
(26) Hodge, I. M. *Macromolecules* **1987**, *20*, 2897.
(27) Hodge, I. M. *Macromolecules* **1983**, *16*, 898.
(28) Hutchinson, J. M.; Ruddy, M. *Makromol. Chem., Macromol. Symp.* **1989**, *27*, 319.
(29) Mercier, J. P.; Aklonis, J. J.; Litt, M.; Tobolsky, A. V. *J. Appl. Polym. Sci.* **1965**, *9*, 447.
(30) Greiner, R.; Schwarzl, F. R. *Rheol. Acta* **1984**, *23*, 378.
(31) Bartos, J.; Müller, J.; Wendorff, J. H. *Polymer* **1990**, *31*, 1678.
(32) Málek, J.; Montserrat, S. *Thermochim. Acta* **1998**, *313*, 191.
(33) Perez, J.; Cavaille, J. Y.; Diaz Calleja, R.; Gómez Ribelles, J. L.; Montleón Pradas, M.; Ribes Greus, A. *Makromol. Chem.* **1991**, *192*, 2141.
(34) Hutchinson, J. M.; Kriesten, U. In *Macromolecules 1992*; Kahovec, J., Ed.; 1993; p 45.
(35) Hutchinson, J. M.; Kriesten, U. *J. Non-Cryst. Solids* **1994**, *172−174*, 592.
(36) Cortés, P. Unpublished data.
(37) Angell, C. A. In *Relaxations in Complex Systems;* Ngai, K. L., Wright, G. B., Eds.; US Department of Commerce: Springfield VA, 1984; p 3.
(38) Hutchinson, J. M. *Polym. Int.* **1998**, *47*, 56.
(39) Hodge, I. M. *J. Res. NIST* **1997,** *102*, 195.
(40) Golden, J. H.; Hammant, B. L.; Hazell, E. A. *J. Appl. Polym. Sci.* **1967**, *11*, 1571.
(41) LeGrand, D. G. *J. Appl. Polym. Sci.* **1969**, *13*, 2129.
(42) Bauwens-Crowet, C.; Bauwens, J. C. *Polymer* **1982**, *23*, 1599.
(43) Adam, G. A., Cross, A.; Haward, R. N. *J. Mater. Sci.* **1975**, *10*, 1582.
(44) Struik, L. C. E. In *Failure of Plastics*; Brostow, W., Corneliussen, R. D., Eds.; Hanser: Munich, Germany, 1986; p 209.

MA981391T